Phenology-informed decline risk of estuarine fishes and their prey suggests potential for future trophic mismatches

Robert J. Fournier[1]*, Tyler C. Marino[1], Stephanie M. Carlson[1], Albert Ruhi[1]

[1] Department of Environmental Science, Policy, and Management, University of California Berkeley, Berkeley, CA 94720

* robertfournier@berkeley.edu

Key Words: Phenology, Population viability analysis, Time series analysis, Estuaries, Food webs.

Data Availability: Data, metadata, and R code necessary to reproduce model results, analyses, and figures are accessible as 'private for peer review' on Dryad (data) and Zenodo (code): http://datadryad.org/stash/share/zfLH561PA-zI0Kf_JAgr9gk9ejY2f3ecASN0zvp_vjM. These data will be released upon acceptance. Raw abundance time series data can be accessed via their collecting agency, the California Department of Fish and Wildlife. For additional exploration and visualization of our results, see the companion 'Bay-Delta Data Explorer' ShinyApp http://12022001delta.shinyapps.io/RFCT_Mismatches_2.

Impact Statement: Increasing risk of trophic mismatch between estuarine fish and their prey highlights the need for finer-scale conservation assessments.

Acknowledgements: We thank Denise Colombano (DSC), Noah Knowles (USGS), and Lisa Lucas (USGS) for providing insight on the ecological dynamics of the San Francisco Estuary. We thank the many field personnel who collected the data for each monitoring program (CDFW Bay Study, IEP Environmental Monitoring Program). Funding for this work was provided by the California Department of Fish and Wildlife grant award Q2196006, "Climate-driven food web mismatches in the San Francisco Estuary".

Abstract

Conservation scientists have long used population viability analysis (PVA) on species count data to quantify trends and critical decline risk, thereby informing conservation actions. These assessments typically focus on single species rather than assemblages and assume that risk is consistent within a given life stage (e.g., across the different seasons or months of a year). However, if risk is assessed at too broad a temporal or spatial scale, it may overlook diverging population declines between predators and prey that disrupt biotic interactions. In this study, we used time-series based PVA for age-0 forage fishes and their potential zooplankton prey for each month of the year in the San Francisco Estuary, over 1995-2023 (N = 175 time series). We used Multivariate Autoregressive (MAR) models that estimate long-term population trends and variability (i.e., process error) for each population. We found widespread negative population trends across fish species (56.6%) and observed that critical decline risk is often higher in months when species abundances peak compared to 'shoulder' months. Although current decline risk is somewhat balanced between predators and their prey (mean 21.8% for fish and 21.4% for zooplankton), our time-series models indicate trophic levels are poised to diverge over the next 10 years, with fish generally accumulating risk faster than their prey. Additionally, zooplankton showed 11.5% higher uncertainty about their near-term critical decline risk relative to fish. These observations suggest strong, previously unreported potential for future trophic mismatches. Our results underscore the need to assess risk over finer temporal scales within and across trophic levels to better understand vulnerability, and thus inform conservation of imperiled species. Our approach is transferable and highlights the benefits of time-series based PVA to understand risk of food-web collapse in the face of climate-induced phenological shifts.

Introduction

Global climate change challenges current efforts to conserve and manage biodiversity (IPBES 2019). Severe population declines and local extirpation can drive permanent shifts in community composition and destabilize whole food webs (O'Gorman and Emmerson 2009, Seifert et al. 2015). Though conservation actions attempting to bolster population recovery are widespread geographically across both animal and plant systems (Swaisgood et al 2007, Mawdsley et al. 2009, Havens et al. 2014), quantifying extinction risk in species with complex life cycles remains challenging (e.g., Sánchez- Hernández et al. 2019, Daly et al. 2021). For instance, determining the effects of a given stressor (e.g., temperature, salinity) on individual survival or performance must account for the differential sensitivities across life stages (Komoroske et al. 2014). Additionally, species phenology (e.g., the timing of migration, breeding, or niche shifts) can cause the strength of important biotic interactions to vary through time and across space (Werner and Gillam 1984). Thus, accounting for community-level dynamics, including how predators and prey coexist in space and time, is essential for improving conservation outcomes of at-risk species.

Population viability analysis (PVA) is a widely used tool to assess threats to species persistence, forecast population trends, and guide recovery (Akçakaya and Sjögren-Gulve 2000). Historically, these models have taken many forms–from demographic assessments, to estimation of minimum viable population sizes, or mechanistic covariate-driven simulations (Gerber and González-Suárez 2010). PVA allows conservation practitioners to assess population performance by estimating the cumulative probability of exceeding a critical decline threshold, often termed ‘quasi-extinction’ (Fagan and Holmes 2006). However, these models generally have strict data requirements and are difficult to effectively parameterize without robust understanding of demographic and environmental processes (Chaudhary and Oli 2020). To circumvent this shortcoming, statistical methods were developed that estimate the convergent properties of stochastic systems and allow for quasi-extinction forecasting even

when the underlying mechanistic processes are poorly understood (Holmes et al. 2007). Such models use repeated sampling of a population (i.e., a time series of count data) to assess inherent growth rates and process-driven population variability. In addition to applications estimating quasi-extinction probabilities under different scenarios (e.g., Ruhi et al. 2016, Ruhi et al 2018), these methods can also infer metapopulation spatial structure and associated risk (e.g., Holmes and Semmens 2004, Ward et al. 2010). Given the increasing availability of long-term biomonitoring data sets, understanding the potential and limitations of statistical approaches to species extinction forecasting is an important endeavor of conservation science.

Despite advances in time series-based PVA, current approaches primarily use annual data (Hampton et al. 2013, Holmes et al. 2014). As such, species with sub-yearly phenological patterns (e.g., hatching dynamics, age-0 migrations; Bogner et al. 2016) might display temporal patterns of critical decline risk not captured by a coarser-scale approach. Moreover, while it is possible to examine species interactions using multivariate time series models (e.g., Hampton et al. 2006, Peterson et al. 2017), estimation of interaction strengths often conflicts with estimation of PVA parameters (i.e., intrinsic growth rate or “lambda”, Holmes et al. 2014). However, food-web dynamics that might be critical to population performance can be assessed indirectly–for instance, by comparing fine-scale patterns of risk of a predator vs that of its prey. While statistically challenging, it is ecologically important to consider decline risk within the context of community-level interactions, especially in environments where population persistence may be influenced by climate-induced changes in species phenology.

Estuaries are dynamic ecosystems with levels of biological productivity comparable to tropical rainforests and coral reefs (Cai 2011). Estuarine systems provide high socioeconomic value, facilitate important ecosystem services, and govern many nearshore physical and biological processes (Barbier et al. 2011, Robins et al. 2016). For many taxa, estuaries often represent important nursery grounds (Beck et al. 2001, Colombano et al. 2020), refuge habitats (Simenstad et al. 1982), and migration corridors (Koeller et al. 2009, Otero et al. 2014).

However, the transitional nature of estuaries makes them highly vulnerable to environmental change, as degradation to both the marine and freshwater bookends have the potential to disrupt estuarine communities (Gillanders et al. 2011, Lauchlan and Nagelkerken 2020). Indeed, many estuarine systems globally are experiencing climate-induced shifts in temperature and salinity regimes that can strongly impact population dynamics (Scanes et al. 2020, Langan et al. 2021, Ghalambor et al. 2021). As estuaries often act as temporary or transitional habitats for key life stages, many taxa have developed population cycles that maintain historical synchrony between interacting species (Marques et al. 2006). However, warming and salinization appear to be altering phenological patterns in estuarine food webs–with the potential to disrupt historically synchronous population cycles between predators and prey (Chevillot et al. 2017, Asch et al. 2019, Fournier et al. 2024). This is especially important for juvenile fishes, as global change drivers that disrupt community compositions could lead to recruitment failures that erode the nursery function of estuarine ecosystems (Colombano et al. 2022).

The San Francisco Estuary is one of the largest and most ecologically significant estuaries in North America, draining approximately 40% of California's fresh waters (Cloern and Jassby 2012). The estuary spans a wide salinity gradient from the Pacific Ocean to the confluence of the Sacramento and San Joaquin rivers, and is highly affected by both hydroclimatic variability and large-scale water diversions for agricultural and municipal use (Reis et al. 2019). In the past decade, the estuary has experienced steadily increasing water temperatures (Bashevkin et al. 2022), and long-term droughts have decreased freshwater inputs into the Delta, resulting in increased salinity levels in the upper estuary (Barros et al. 2024). Additionally, invasions of Asian clams (*Potamocorbula amurensis* and *Corbicula fluminea*) in the late 1980's dramatically eroded planktonic populations (Kimmerer et al. 1994), leading to dietary shifts of planktivores (Feyrer et al. 2003). These and other environmental changes have resulted in large-scale collapses of pelagic fish populations throughout the estuary (Cloern and Jassby 2012, Quiñones and Moyle 2014). Often referred to as the "pelagic

organism decline", forage fish populations have shown precipitous drops even during periods of relatively moderate abiotic stress (Sommer et al. 2007). Though the mechanistic causes of this decline remain poorly understood, recruitment failure, increased mortality, habitat degradation, and limited food availability have been identified as main drivers–especially for juvenile forage fish (Sommer et al. 2007, Feyrer et al. 2007, Mac Nally et al. 2010). These concerning trends underscore the need to better understand the dynamics of forage fishes in the first year of their life (i.e., age-0), as well as of their food sources.

Here, we sought to assess spatial and temporal patterns of critical decline risk of fish, and their suite of potential prey in the San Francisco Estuary. As age-0 estuarine fishes display seasonally varying abundance patterns that might coincide with periods of population vulnerability, we sought to examine critical decline risk at sub annual scales. To that end, we used long-term monitoring data to conduct time-series based PVA for each month of the year for age-0 forage fishes and zooplankton taxa across different regions of the San Francisco Estuary spanning a broad environmental gradient. We hypothesized that: 1) Long-term population trends and variability around those trends would vary across fish species, creating ample variation in the probability of them crossing critical decline thresholds (hereafter, *critical decline risk*); 2) Critical decline risk in a given species would also vary across the year, with months that historically concentrated high abundance of age-0 being relatively safer than "shoulder" months when species have historically shown lower abundances; 3) Patterns of critical decline risk–and uncertainty around risk estimates–during high abundance windows might differ between fish predators and their potential suite of prey, and this risk might accumulate at different rates over the next decade as steep population declines in fishes might cause risk to outpace zooplankton taxa; And 4) Different regions of the estuary may vary in community-level risk trends, with variation likely being associated with the longitudinal estuarine gradient (i.e., higher in more variable, seawards regions than in more stable, landwards regions). By examining these questions, we aimed to understand how critical decline risk of

estuarine fishes may vary intra-annually and over space–a critical step to anticipate vulnerability of predator-prey interactions along environmental gradients.

Methods

Fish and plankton surveys

We gathered long-term monitoring data for fishes and zooplankton in the San Francisco Estuary. For fishes, we used data provided by the California Department of Fish and Wildlife Bay Study (CDFW 2024a). This program has conducted monthly sampling of fishes at fixed stations throughout the estuary since 1980. Fish sampling is conducted using two tow nets: an otter trawl to target benthic species and a midwater trawl to target pelagic species. During each sampling event, captured individuals are counted, identified, and measured. Additionally, sampling effort is quantified to standardize catch metrics. Our analysis focused on age-0 fishes captured in the midwater trawl. For zooplankton, we used data collected by the Interagency Ecological Program's Environmental Monitoring Program, EMP (CDFW 2024b). The EMP has been sampling zooplankton at fixed stations monthly since 1971, using three types of sampling gear: a macrozooplankton net (505 µm mesh), a mesozooplankton net (160 µm mesh), and a teel pump with 43 µm mesh. In order to target taxa that might be readily consumed by age-0 forage fishes, we limited our analysis to zooplankton captured in the mesozooplankton net. We filtered each time series to include only monthly surveys after January 1995, as this period maximizes overlap in consistent sampling of fish and zooplankton.

Data screening

We assessed data completeness iteratively, to achieve an optimal tradeoff between maximizing data density in the species-stations retained, and avoiding exclusion of transient or migratory fishes that are only seasonally present in parts of the estuary. We ultimately retained time series with 234 and 50 non-zero detections for zooplankton and fishes, respectively. We

then calculated high abundance for each fish species by identifying the months that represent most of the mean annual catch for that species in a region (≥80%). In situations where critical periods contained gaps of no more than one month, we also included the 'skipped' month to obtain an uninterrupted window. Next, for each species-station strata, we used seasonal autoregressive integrated moving average (sARIMA) models fitted with a Kalman filter to interpolate missing monthly data points (as in Comte et al. 2021), using the 'forecast' package in R (Hyndman et al. 2024). Interpolated data represented an average of 20.3% data points for fish taxa and 3.1 % for zooplankton. This process resulted in 7 fish species being retained across 52 stations, and 10 zooplankton genera at 16 stations. Fish and zooplankton stations were assigned to predefined estuarine regions that have been commonly used for research and management purposes, encompassing from the marine to the freshwater bookend (CDFW 2024a, Colombano et al. 2022). In four of the estuarine regions (i.e., *Delta, Confluence, Suisun, San Pablo*), both fish and potential zooplankton prey were retained. Finally, we broke each year into its constituent months to create twelve annual-scale, month-specific time series for each species/station pair (i.e., one time series representing all January data for each year, one representing February data, etc.). For subsequent analysis on phenology-informed risk (see below), we kept all species-station-month strata as long as a species was historically present with some regularity (i.e., in ≥30% of the years), achieving higher retention rates than in past work (e.g. Colombano et al. 2021, Pak et al. 2022). Ultimately, we ended up with 129 time series of fish and 46 of zooplankton, each relevant to a specific station and month.

Time series modeling and risk calculation

With these time series, we fitted Multivariate Autoregressive (MAR) models on CPUE estimates using the R "MARSS" package (Holmes et al. 2014). Here, we used the multivariate structure of MAR models to describe population trajectories within regions. Thus, after grouping

the 62 stations into 6 regions, we built a MAR model for each species-region-month strata. MAR models, unlike state-space variations of them (e.g. MARSS), do not account for observation error. We acknowledge that observation error is prevalent in biomonitoring data, and metrics dependent on process error might be inflated if process error is forced to absorb observation error (Knape and De Valpine 2011). However, variation in data density prevented more complex (MARSS) models from converging for some species. Thus, we sought to maintain consistency in bias rather than accounting for observation error in some species, which could bias some (but not all) risk estimates and thus mismatch potential. The general structure of our MAR models, in matrix notation, followed:

$$X_t = X_{t-1} + U + W_t,\ where\ W_t \sim MVN(0, Q), \text{ (Eq. 1)}$$

where X_t is log x+1 transformed CPUE for that species (one time series per station, univariate or multivariate depending on how many stations are represented in that region); *U* captures the long-term trend of that regional population, and W_t is an error term drawn from a multivariate normal distribution of mean 0 and process error variance/covariance *Q*. For all models, we estimated a single *U* across stations within a region. Similarly, we assumed process error variance to be equal across stations, and we allowed process error covariance given that nearby stations are subject to similar environmental fluctuations that could drive synchronous population dynamics within a region. After estimating *U* and *Q* via maximum-likelihood (and obtaining 95% confidence intervals for each parameter), we calculated the risk of a species experiencing a 90% population decline (a) over a given time horizon (*T*) up to 10 years from present. This quasi-extinction probability (P_e), hereafter referred to as 'critical decline risk', is estimated by using the inverse Gaussian distribution of first passage times for Brownian motion with drift (Dennis et al. 1991, Fieberg and Ellner 2000, See and Holmes 2015), where:

$$P_e = \phi(\mu - V) + exp(2\mu V)\phi(-(\mu - V)), \text{ (Eq. 2)}$$

$$\mu = -U\sqrt{T/Q}, \text{ (Eq. 3)}$$

$$V = a/Q\sqrt{T}, \text{ (Eq. 4)}$$

with ϕ representing the standard normal cumulative distribution function (notation in the above equations have been modified to maintain consistency with MAR parameter notation). Here, we calculated three different types of critical decline risk: 1) *baseline risk,* using the maximum likelihood estimates for *U* and *Q*; 2) *best case-scenario risk*, using the upper end of the bootstrapped confidence interval for *U*, and the lower end of the confidence interval surrounding *Q* (i.e., high growth rate and low process error variance), and 3) *worst-case scenario risk*, using the lowest end of the confidence interval surrounding *U* and the highest end of the confidence interval surrounding *Q* (i.e., low or negative intrinsic growth, high process error variance).

Hypothesis testing

To test the hypothesis that long-term population trends (*U*) and variability around those trends (*Q*) would vary across fish species, we plotted *U* and *Q* values estimated by MAR models and tested whether systematic differences existed across fish *species* and *regions*, using analysis of variance (ANOVA). We also examined the correlation (Pearson's R) between these two parameters to understand whether species with declining trends tended to also be more variable, or if on the contrary, *U* and *Q* varied independently across species and regions.

To test the hypothesis that critical decline risk in a given species would also vary across the year, we assessed the "phenology" of critical decline risk throughout the year for age-0 forage fishes by plotting monthly risk estimates for each species in each region. We then performed Pearson correlation tests between decline risk and mean population size for each species, pooling data across regions, to assess if these two variables were related–and if so, whether 'shoulder' months tended to be safer than months when species have historically shown higher abundances (or *vice versa*).

To compare how critical decline risk compares between fish (predators) and their suite of zooplankton prey, we examined current critical decline risk during key months of the year (i.e.,

the months that collectively concentrate 80% of a species' abundance). To this end, we calculated the mean risk for all months identified as high abundance windows for each region. In addition, we calculated the mean decline risk for each zooplankton during the high abundance window of each fish predator–creating paired predator/prey probabilities in each region. To assess if predator and prey risk during high-abundance windows differed, we used ANOVA, using "current" critical decline risk (that is, the probability of crossing an 90% decline threshold) as a response variable, and taxonomic *group* (fish or zooplankton) and *region* (if present in more than one region) as predictors. We ran an ANOVA model for each fish species and its paired assemblage of potential zooplankton prey.

To test whether risk is predicted to accumulate at different rates between fish and zooplankton over the next decade, we calculated predator-prey risk divergence into the future for each predator and their set of prey (as previously) across a 10-year projection. Using analysis of covariance (ANCOVA), we tested whether log-transformed risk was explained by taxonomic *group* (fish *vs.* zooplankton) and/or *region*, using *time* into the future as a covariate (i.e., number of *years*, 1-10). We also considered potential interactions between these terms. A significant interaction between *time* and *group* would indicate a widening (or closing) gap between predator and prey risk—implying mismatch potential. Triple interactions between *time*, *group*, and *region* allowed testing whether diverging gaps in risk between fish and their prey were region-specific. This analysis also allowed assessing how trends might scale up to the broader regional food webs across the estuary, by modeling risk estimates for the whole community as a function of taxonomic *group*, *time*, *region*, and *predator* identity (to cluster individual food webs). Finally, we used the same ANCOVA model structures to estimate the difference in risk between "best case" and "worst case" scenarios. This last analysis allowed for assessing the implications of assuming trends (U) and process error (Q) on the lower or higher ends that the data supported–and thus the conservation implications of population uncertainty.

Results

Quantifying population trends and variability

Maximum-likelihood estimates of fish intrinsic growth rates (or long-term population trends, *U*), and of process error variance (or variability around the long-term trends, *Q*) revealed a wide diversity of trajectory types across species (Figure 3). These variables showed no strong association with each other (Pearson's R: 0.133, p=0.053). We tended to see negative growth rates (mean ± SD: -0.009 ± 0.0763) that varied by *species* ($F_{6,26.535}$, p<0.001) and by *region* ($F_{5,2.715}$, p=0.021). However, positive population trajectories were also possible (positive: 42.4%, negative: 56.6%, range: -0.210 to +0.176). Process error variance, which measures the inherent variability of the population associated with environmental stochasticity, varied strongly by *species* ($F_{6,49.994}$, p<0.001), *region* ($F_{5,18.761}$, p<0.001), and the interaction between *species* and *region* ($F_{10,5.364}$, p<0.001). Notably, Longfin Smelt (*Spirinchus thaleichthys*) displayed nearly ubiquitous declining trajectories and had relatively small levels of process error variance. Conversely, Northern Anchovy (*Engraulis mordax*) showed more positive population growths, but did so with very high levels of process error variance (Figure 3). Overall, in agreement with our hypothesis, we observed wide variation in population risk, driven by both spatial variation (regions) and individual species characteristics.

Phenology of risk

Fishes showed fluctuating patterns of critical decline risk throughout the year, despite critical decline risks being low overall (mean: 20.6%) (Figure 4). Moreover, taxa in regions at the high end of the salinity gradient (i.e., San Pablo Bay) often were at higher mean risk (San Pablo Bay = 21.6%) than those in lower salinity zones (Delta=16.1%, Confluence = 16.8%, Suisun Bay = 14.0%). We also modeled risk dynamics in the high-salinity zones of the Central and South Bays, and found high mean risk probabilities (Central 30.4%, South 25.6%, Supplementary Figure S3). However, as these regions do not have zooplankton monitoring, we

312 excluded them from additional analysis. Critical decline risk was positively correlated with mean
313 monthly abundance of age-0 American Shad (*Alosa sapidissima*), Pacific Herring (*Clupea*
314 *pallasii*), Striped Bass (*Morone saxatilis*), Threadfin Shad (*Dorosoma pretense*), and Longfin
315 Smelt populations (American Shad R=0.5792, $T_{27,3.6926}$, p<0.001, Pacific Herring R=0.7642,
316 $T_{8,3.3517}$, p=0.01, Striped Bass R=0.5453, $T_{33,3.7368}$, p<0.001, Threadfin Shad R=0.5887, $T_{20,3.2573}$,
317 p=0.004, Longfin Smelt R=0.6155, $T_{20,3.4929}$, p=0.002). This result indicates that critical decline
318 risk is often higher in months that concentrate higher abundances. In contrast, the Jack
319 Silverside (*Atherinopsis californiensis*) and the Northern Anchovy did not show an association
320 between month-specific risk and abundance. Notably, no species showed a negative
321 association between monthly risk and abundance–the hypothesized pattern in which species
322 would be safer in the months that concentrate more of their relative abundance, relative to the
323 'shoulder' months.
324
325 *Implications for trophic dynamics in current and future scenarios*
326 We found that critical decline risk was relatively low (mean 21.46%) when we examined
327 paired predator-prey assemblages within their high-abundance windows one time step into the
328 future (Figure 5). Though individual zooplankton taxa showed variable patterns of risk in the
329 near term, only one predator, the Striped Bass, showed significantly lower decline risk than its
330 corresponding prey assemblage ($F_{1,17.320}$, p=0.0015), indicating potential for bottom-up
331 destabilization. Additionally, American Shad predator/prey assemblages showed differential
332 patterns by region, with lower critical decline risks associated with San Pablo Bay ($F_{3,8.601}$,
333 p=0.002).
334 Despite this 'balanced' risk between fish and their prey currently, as we projected critical
335 decline risk into the next decade we found widespread divergence between fishes and their
336 zooplankton prey across different regions of the estuary ($F_{3,4.068}$, p=0.006 for the
337 Group*Time*Region interaction, see next section for community-level trends). Among individual

predators, all fish species except the Threadfin Shad displayed differential risk than their prey assemblages (Figure 6), but this often varied by region. Notably, Striped Bass also displayed an interaction between taxonomic group and years into the future, indicating that risk accumulates at different rates between this fish and its prey ($F_{1,14.581}$, p<0.001). Throughout the 10-year projection, we also found strong regional differences in American Shad ($F_{3,39.422}$, p<0.001), Northern Anchovy ($F_{1,16.407}$ p<0.001), and Longfin Smelt food webs ($F_{1,6.705}$ p=0.0109), as well as *group* by *region* interactions for all three of these predators (American Shad $F_{3,8.132}$, p<0.001; Northern Anchovy $F_{1,5.577}$, p=0.02; Longfin Smelt $F_{1,5.932}$, p=0.016). Additionally, we found that American Shad food webs accumulate risk differentially by region ($F_{3,10.060}$, p<0.001 for the *region* by *time* interaction). Overall, we saw support for our hypothesis that fishes display higher levels of risk than their zooplankton prey into the future, but these trends are largely region-specific.

Community-scale observations

Divergences between fish and zooplankton critical decline risks also manifested at the community level, with zooplankton assemblages throughout the estuary having lower mean decline risk than fishes ($F_{1,7.022}$, p=0.008). However, these differences are predominantly driven by patterns in San Pablo Bay (Region effect $F_{3,23.168}$, p<0.001, Figure 7). Moreover, we found the rate of divergence in trends through time was unique each region of the estuary ($F_{3,4.068}$, p=0.006 for the *group*time*region* interaction), as well as unique to each predator/prey assemblage ($F_{3,2.715}$, p=0.013 for the triple interaction between *group, time,* and *predator identity*). Despite the higher baseline critical decline risk in fish assemblages, uncertainty (i.e., the difference between risk from best-case and worst-case scenario projections) was higher for zooplankton relative to fish ($F_{1,113.867}$, p<0.001), and accumulated differently between trophic groups ($F_{1,17.060}$, p<0.001 for the *group* by *time* interaction). Moreover, uncertainty varied by *region* ($F_{3,121.889}$, p<0.001), and *groups* in each *region* accumulated risk differentially through

time ($F_{3,7.201}$, p<0.001 for the triple interaction between *group, time,* and *region*). This interaction indicates that a wider range of critical decline outcomes are possible for zooplankton across the estuary. Overall, these results suggest that patterns of risk can scale up from individual predator/prey assemblages to the community level. However, local conditions–notably the salinity gradient–control how these patterns might manifest into the future. For additional exploration and visualization of our results, see the companion 'Bay Delta Data Explorer' R ShinyApp: http://12022001delta.shinyapps.io/RFCT_Mismatches_2.

Discussion

Conservation scientists often quantify extinction risk to triage populations and prioritize the allocation of limited resources. However, these estimates often assume that decline risk is consistent within relatively small temporal and spatial scales (Coulson et al. 2001). Moreover, PVA are usually explored within the context of a single species, and assessments of risk across food webs is comparatively rare (Sabo 2008). Here, we sought to evaluate how critical decline risk for age-0 forage fishes and their potential prey varies throughout the year across the San Francisco Bay Estuary. Both forage fishes and their zooplankton prey were characterized by periods of concentrated abundance within years, emphasizing the importance of considering decline risk at sub-yearly scales. We found that many focal fish species showed negative population growth, and that critical decline risk was often higher in months with high historical abundances. Additionally, we found that predator and prey decline risk diverged across a 10-year projection, suggesting a potential for future trophic mismatches. However, these divergent patterns were most pronounced in one region of the estuary (San Pablo Bay), indicating that local environmental factors might drive disruptions to the food web. Our findings underscore the need to consider fine-scale temporal and spatial variation in risk in estuarine taxa. The observed widening gaps in risk and uncertainty around risk between trophic levels advance the notion that phenological shifts and associated trophic mismatches are an

emergent, yet largely underappreciated consequence of global change on ecological communities (Cohen et al. 2018, Fournier et al 2023).

Widely declining fish population trajectories

There is growing evidence that the capacity of the San Francisco Estuary to support forage fish populations has substantially diminished in recent decades (Rosenfield and Baxter 2011). The resulting pelagic organism decline (POD) has been marked by dramatic collapses in forage fish populations (Sommer et al. 2007), and these declining abundances are reflected across our MAR models (Figure 3). Previous applications of time series modeling in this system have identified strong negative trends at the population level driven by a variety of environmental factors, including water clarity and the variable position of the 2‰ isohaline zone, X_2 (Mac Nally et al. 2010). Understanding the causes and consequences of these declines requires linking abundance trends to probabilistic estimates of extinction outcomes.

Our critical decline risk calculations are based on two primary measures of population dynamics: intrinsic growth rates and process-driven variability. Over half of all fish time series (52.3%) displayed negative intrinsic growth rates, commonly resulting in increased critical-decline risk—that is, a high near-term probability that the species will not be longer present, that month, in that region of the estuary. Notably, the Longfin Smelt, a native osmerid that was historically abundant in the San Francisco Estuary (Tempel et al. 2021), exhibited nearly ubiquitous patterns of negative growth across regions and months (Figure 3). Declines of Longfin Smelt are well established (Nobriga and Rosenfield 2016), and habitat degradation and successive recruitment failures have led to its recent Federal listing under the Endangered Species Act (USFWS 2024). In this case, the strongly negative growth rates identified by our models likely drive the observed patterns of critical decline risk. Conversely, taxa with highly variable population dynamics can still exhibit high decline risk even with positive growth trends. For instance, the Northern Anchovy often maintained positive growth rates but did so in a highly

variable manner (Figure 3). This predominantly marine species opportunistically uses estuarine habitats (Allen and Horn 2006). Populations tend to show boom-and-bust dynamics, with recruitment often tied to lower delta outflow, and juvenile abundance positively correlating with drought conditions that increase system salinity (Colombano et al. 2022). A strong reliance on environmental stochasticity to maintain abundance levels is reflected in high population variance, increasing the likelihood of a critical decline event. Overall, both the overall negative growth rates and high population variance identified by our time series models illustrate an assemblage in flux.

Phenology of risk

Fish recruitment to adult life stages (and fisheries) is often highly sensitive to fluctuations in early life survivorship (Hjort 1914, Winemiller and Rose 1992, Fournier et al. 2021), and our models revealed that age-0 critical decline risk was not uniform across months. The dynamic environmental conditions of estuaries can disproportionately impact juvenile fishes that rear in these nursery habitats (Morrongiello et al. 2014, Jenkins et al. 2022). For example, seasonal changes in delta outflow and salinity can alter resource availability during key growth periods (Reis et al. 2019). Additionally, widespread anthropogenic alteration of breeding and rearing habitats throughout the San Francisco Estuary has negatively affected early life stages of estuarine fishes (Cloern and Jassby 2012). Despite our expectation that critical decline risk would be higher during months with historically low abundances, we often observed the opposite pattern. American Shad, Longfin Smelt, Pacific Herring, Striped Bass, and Threadfin Shad all showed higher critical decline risks in months with historically high abundances. Low juvenile survivorship often leads increased fecundity, to buffer mortality (Winemiller and Rose 1993), which likely explains the observed risk patterns. Moreover, density-dependent resource exploitation during high abundance windows might affect population performance more acutely than density-independent factors in other parts of the growth season (DeAngelis et al. 1993).

Spawning and hatching are key phenological events, the timing of which tends to be highly-sensitive to environmental change (Lawrence et al. 1997, Hovel et al 2017). Our analyses and risk estimates focused on these high-abundance windows. If environmental conditions during these periods become unsuitable, estuarine taxa might respond by advancing or delaying their life cycles their phenology (Chevillot et al. 2017, Asch et al. 2019). However, estuarine fishes might be limited in their abilities to phenologically track changing environmental conditions long-term (Fournier et al. 2024). Moreover, desynchronization between a population and its key resource base can destabilize food webs (Stenseth and Mysterud 2002, Zhemchuzhnikov et al. 2021). Our results highlight the need to closely monitor decline risk during the key periods when a species is present, as assuming risk consistency could mislead managers to overlook potentially impactful moments of heightened risk.

A widening gap in risk, and risk uncertainty, between fishes and their prey

While PVA are generally considered within single species contexts, we sought to pair predators with their potential prey assemblage during important phenological windows. Though near-term patterns of decline risk were similar between predators and their prey, we observed that risk diverged when considering a 10-year time horizon. Predators and prey often fluctuate together in lagged cycles (Chesson 1978) and typically reach equilibrium over evolutionary timescales (Smith and Slatkin 1973). While predictable disturbances can stabilize trophic interactions (Vasseur and Fox 2009), strong environmental fluctuations driven by global change might disrupt these relationships (Bretagnolle and Gills 2010). Additionally, phenological shifts that decouple historically synchronous species can cause trophic mismatches that destabilize food webs (Varpe et al. 2010, Thakur 2020), and phenological trends between estuarine predators and prey could be diverging (Fournier et al. 2024).

Our projections indicated that predators often exhibited higher rates of decline than their prey over a 10-year period. If predators are extirpated during key phenological windows while

their prey persist, the resulting trophic release of zooplankton taxa might increase the likelihood of harmful algal blooms (Jachowski et al. 2020). Conversely, Striped Bass, a non-native but well-established species in the San Francisco Estuary, often showed lower critical decline risk than its prey. Despite its high diet adaptability (Young et al. 2022), significant declines in prey assemblages during key phenological periods might still result in population declines (Nobriga and Freyer 2008). Indeed, altered patterns of prey availability are thought to be a significant driver of the estuary's pelagic organism decline (Sommer et al. 2007). Importantly, we observed different levels of risk uncertainty (i.e., the difference between best-case and worst-case scenarios) between fishes and zooplankton throughout the estuary. In general, zooplankton exhibited a wider range of possible trajectories than fishes. The fast generation times and boom-and-bust cycles characteristic of many zooplankton taxa, including the widespread genera examined in our model, complicate precise estimates of decline risk (Lane 1975). Moreover, biotic controls on plankton populations not assessed by our models (e.g., grazing pressure by invasive bivalves, Carlton et al. 1990) might further destabilize zooplankton prey pools. Thus, while the aggregate stability of the assemblage might facilitate prey-switching (Potts et al. 2016), large-scale collapses predicted by our "worst-case" models would likely destabilize whole food webs.

In our study, we found that the strongly divergent trends (i.e., "widening risk gaps" between fishes and their prey) occurred in a single region of the estuary, San Pablo Bay. This region is near the Pacific Ocean and has the highest salinity levels in the study area. Consequently, long-term droughts that shift the salinity gradient upriver, coupled with the influence of recent marine heatwaves, might make this region especially vulnerable to hydroclimatic fluctuations (Sanford et al. 2019). As fishes and plankton have variable tolerances to environmental conditions such as increased temperature or salinity (Qasim et al. 1972, Beitinger et al. 2000), harsher conditions in this region might differentially influence decline risk. Although individual taxa might display variable levels of risk, a diversity of trends might promote

community-level stability (Ovaskainen et al. 2010). At the estuary-wide scale, the taxonomic richness of forage fishes appears to facilitate portfolio effects that enhance community resilience despite declines of individual taxa (Colombano et al. 2022). Additionally, spatial insurance may allow individual subregions to bolster the metapopulation when local conditions become unsuitable elsewhere. Indeed, previous time series analyses have been used to infer metapopulation structure and identify subpopulations that disproportionately impact regional decline risk (Ward et al. 2010, Sarremejane et al. 2021). Similarly, except for Striped Bass, the divergent patterns we observed in San Pablo Bay appear to be localized, as other subregions throughout the estuary show similar risk for fishes and their prey. Thus, management strategies that either mitigate risk in San Pablo Bay, or enhance the capacity of other subregions to serve as refuge habitats, might confer food-web stability throughout the region.

Limitations and future directions

The increasing availability of biological monitoring data makes time series-based approaches a suitable alternative to traditional, mechanistic PVA (Holmes et al. 2007, Chaudhary and Oli 2020). Here, we leveraged long-term monitoring data for age-0 forage fishes and their zooplankton prey in the San Francisco Estuary to assess critical decline risk across multiple scenarios. Nonetheless, these methodologies have limitations. First, here we explored sub-annual trends by breaking the time series into its constituent months. While this fine-scale analysis revealed when in a given season a particular fish may be more likely to disappear, we did not explicitly model spawning and hatching events, niche shifts, or migrations. Additional work could build on our approach to mechanistically include life-history events that may be influencing, or driving, the observed patterns in risk phenology. Second, our critical decline metrics might be inflated because they are derived solely from process error while observation error is not assessed (Knape and De Valpine 2011). However, these estimates remain valuable because our modeling approach promotes bias consistency across fish species and their

potential prey. Furthermore, the probability of not detecting a species in a given month (i.e., 'extinction' from an observation standpoint) is still critical, as it may prompt management and conservation actions, even if the species was not detected due to imperfect observation rather than true absence (e.g., Delta Smelt, Rose et al. 2013). Third, direct biotic interactions are difficult to estimate. We sought to ameliorate this shortcoming by calculating average risk of prey within phenological windows bespoke to each predator. However, these indirect methods might not fully assess increases in decline risk due to prey availability, and altered prey pools are predicted to influence pelagic organism population collapses (Sommer et al. 2007, Cloern and Jassby 2012). Moreover, while we assumed fishes might consume any of the modeled prey species, we still know relatively little about how each fish predator might rely on a given prey item. Thus, diet and other trophic studies that directly link predator and prey would greatly improve our ability to assess mismatch potential. Finally, our models examined spatial dynamics by assessing decline risk at subregional scales. In doing so, we found that San Pablo Bay has elevated mismatch risk relative to other regions of the estuary. As migration through the estuary is common for many of our focal taxa, explicit examinations of metapopulation structure might enhance our understanding of whole-estuary ecological dynamics.

Concluding remarks

The richness and complex life cycles of estuarine biota often complicate management and conservation efforts in these dynamic ecosystems (Jha et al. 2008, Lauchlan and Nagelkerken 2020). Here, we used a novel quantitative approach to estimate critical decline risk in a community context. Contrary to what is typically assumed, we found that even within a given species and life stage, critical decline risk can be highly variable across months of the year–suggesting high potential for climate-induced trophic mismatches (Visser 2022). Because predator-prey dynamics and food limitation have been linked to the ongoing fish population declines in the San Francisco Estuary (Baxter et al. 2008, Cloern & Jassby 2012), our results

546 are directly relevant to conservation efforts in this system. Notably, our approach could be
547 transferred to other estuaries with similar long-term on species abundances across trophic
548 levels. A more robust understanding of fine-scale temporal dynamics within food webs should
549 help design more effective conservation strategies for vulnerable populations undergoing
550 climate-change induced phenological shifts.
551

References

Akçakaya, H. R., & Sjögren-Gulve, P. (2000). Population viability analyses in conservation planning: An overview. *Ecological Bulletins*, 9–21.

Allen, L. G., Pondella, D. J., & Horn, M. H. (2006). *The ecology of marine fishes: California and adjacent waters*. Univ of California Press.

Asch, R. G., Stock, C. A., & Sarmiento, J. L. (2019). Climate change impacts on mismatches between phytoplankton blooms and fish spawning phenology. *Global Change Biology*, *25*(8), 2544–2559.

Barbier, E. B., Hacker, S. D., Kennedy, C., Koch, E. W., Stier, A. C., & Silliman, B. R. (2011). The value of estuarine and coastal ecosystem services. *Ecological Monographs*, *81*(2), 169–193.

Barros, A., Hartman, R., Bashevkin, S. M., & Burdi, C. E. (2024). Years of Drought and Salt: Decreasing Flows Determine the Distribution of Zooplankton Resources in the San Francisco Estuary. *San Francisco Estuary and Watershed Science*, *22*(1).

Bashevkin, S. M., Mahardja, B., & Brown, L. R. (2022). Warming in the upper San Francisco Estuary: Patterns of water temperature change from five decades of data. *Limnology and Oceanography*, *67*(5), 1065–1080.

Baxter, R., Breuer, R., Brown, L., Chotkowski, M., Feyrer, F., Gingras, M., Herbold, B., Mueller-Solger, A., Nobriga, M., & Sommer, T. (2008). Pelagic organism decline progress report: 2007 synthesis of results. *Interagency Ecological Program for the San Francisco Estuary. Retrieved on May*, *7*, 2011.

Beck, M. W., Heck, K. L., Able, K. W., Childers, D. L., Eggleston, D. B., Gillanders, B. M., Halpern, B., Hays, C. G., Hoshino, K., Minello, T. J., & Orth, R. J. (2001). The identification, conservation, and management of estuarine and marine nurseries for fish and invertebrates: A better understanding of the habitats that serve as nurseries for marine species and the factors that create site-specific variability in nursery quality will improve conservation and management of these areas. *Bioscience*, *51*(8), 633–641.

579 Beitinger, T. L., Bennett, W. A., & McCauley, R. W. (2000). Temperature tolerances of North
580 American freshwater fishes exposed to dynamic changes in temperature. *Environmental*
581 *Biology of Fishes*, *58*, 237–275.

582 Bogner, D. M., Kaemingk, M. A., & Wuellner, M. R. (2016). Consequences of hatch phenology
583 on stages of fish recruitment. *PloS One*, *11*(10), e0164980.

584 Bretagnolle, V., & Gillis, H. (2010). Predator–prey interactions and climate change. *Effects of*
585 *Climate Change on Birds*, 227–248.

586 Cai, W.-J. (2011). Estuarine and coastal ocean carbon paradox: CO2 sinks or sites of terrestrial
587 carbon incineration? *Annual Review of Marine Science*, *3*(1), 123–145.

588 Carlton, J. T., Thompson, J. K., Schemel, L. E., & Nichols, F. H. (1990). Remarkable invasion of
589 San Francisco Bay (California, USA) by the Asian clam Potamocorbula amurensis. I.
590 Introduction and dispersal. *Marine Ecology Progress Series*, 81–94.

591 CDFW a. 2024. California Department of Fish and Wildlife San Francisco Bay study: Long-term
592 fish and water quality monitoring data. https://filelib.wildlife.ca.gov/Public/BayStudy/

593 CDFW b. 2024. Interagency Ecological Monitoring Program. https://iep.ca.gov/Science-
594 Synthesis-Service/Monitoring-Programs/EMP

595 Chaudhary, V., & Oli, M. K. (2020). A critical appraisal of population viability analysis.
596 *Conservation Biology*, *34*(1), 26–40.

597 Chesson, P. (1978). Predator-prey theory and variability. *Annual Review of Ecology and*
598 *Systematics*, *9*, 323–347.

599 Chevillot, X., Drouineau, H., Lambert, P., Carassou, L., Sautour, B., & Lobry, J. (2017). Toward
600 a phenological mismatch in estuarine pelagic food web? *PloS one*, *12*(3), 0173752.

601 Cloern, J. E., & Jassby, A. D. (2012). Drivers of change in estuarine-coastal ecosystems:
602 Discoveries from four decades of study in San Francisco Bay. *Reviews of Geophysics*,
603 *50*(4).

604 Cohen, J. M., Lajeunesse, M. J., & Rohr, J. R. (2018). A global synthesis of animal phenological
605 responses to climate change. *Nature Climate Change*, *8*(3), 224-228.

606 Colombano, D. D., Carlson, S. M., Hobbs, J. A., & Ruhi, A. (2022). Four decades of climatic
607 fluctuations and fish recruitment stability across a marine-freshwater gradient. *Global*
608 *Change Biology*, *28*(17), 5104–5120.

609 Colombano, D. D., Manfree, A. D., Teejay, A. O., Durand, J. R., & Moyle, P. B. (2020).
610 Estuarine-terrestrial habitat gradients enhance nursery function for resident and transient
611 fishes in the San Francisco Estuary. *Marine Ecology Progress Series*, *637*, 141–157.

612 Coulson, T., Mace, G. M., Hudson, E., & Possingham, H. (2001). The use and abuse of
613 population viability analysis. *Trends in Ecology & Evolution*, *16*(5), 219–221.

614 Daly, R., Filmalter, J. D., Peel, L. R., Mann, B. Q., Lea, J., Clarke, C. R., & Cowley, P. D. (2021).
615 Ontogenetic shifts in home range size of a top predatory reef-associated fish (Caranx
616 ignobilis): Implications for conservation. *Marine Ecology Progress Series*, *664*, 165–182.

617 DeAngelis, D., Shuter, B., Ridgway, M., & Scheffer, M. (1993). Modeling growth and survival in
618 an age-0 fish cohort. *Transactions of the American Fisheries Society*, *122*(5), 927–941.

619 Dennis, B., Munholland, P. L., & Scott, J. M. (1991). Estimation of growth and extinction
620 parameters for endangered species. *Ecological Monographs*, *61*(2), 115–143.

621 Fagan, W. F., & Holmes, E. (2006). Quantifying the extinction vortex. *Ecology Letters*, *9*(1), 51–
622 60.

623 Feyrer, F., Cloern, J. E., Brown, L. R., Fish, M. A., Hieb, K. A., & Baxter, R. D. (2015). Estuarine
624 fish communities respond to climate variability over both river and ocean basins. *Global*
625 *Change Biology*, *21*(10), 3608–3619.

626 Fieberg, J., & Ellner, S. P. (2000). When is it meaningful to estimate an extinction probability?
627 *Ecology*, *81*(7), 2040–2047.

628 Fournier, R. J., Bond, N. R., & Magoulick, D. D. (2021). Modeling effects of disturbance across
629 life history strategies of stream fishes. *Oecologia*, *196*(2), 413–425.

630 Fournier, R. J., Colombano, D.D, Latour, R.J., Carlson, S.M., & Ruhi, A. (2024).
631 Modeling effects of disturbance across life history strategies of stream fishes. *Ecology*
632 *Letters*, *27:e14441*

633 Gerber, L. R., & González-Suárez, M. (2010). *Population viability analysis: Origins and*
634 *contributions*.

635 Ghalambor, C. K., Gross, E. S., Grosholtz, E. D., Jeffries, K. M., Largier, J. K., McCormick, S.
636 D., Sommer, T., Velotta, J., & Whitehead, A. (2021). Ecological effects of climate-driven
637 salinity variation in the San Francisco Estuary: Can we anticipate and manage the
638 coming changes? *San Francisco Estuary and Watershed Science*, *19*(2).

639 Gillanders, B. M., Elsdon, T. S., Halliday, I. A., Jenkins, G. P., Robins, J. B., & Valesini, F. J.
640 (2011). Potential effects of climate change on Australian estuaries and fish utilising
641 estuaries: A review. *Marine and Freshwater Research*, *62*(9), 1115–1131.

642 Hampton, S. E., Holmes, E. E., Scheef, L. P., Scheuerell, M. D., Katz, S. L., Pendleton, D. E., &
643 Ward, E. J. (2013). Quantifying effects of abiotic and biotic drivers on community
644 dynamics with multivariate autoregressive (MAR) models. *Ecology*, *94*(12), 2663–2669.

645 Hampton1, S. E., Scheuerell, M. D., & Schindler, D. E. (2006). Coalescence in the Lake
646 Washington story: Interaction strengths in a planktonic food web. *Limnology and*
647 *Oceanography*, *51*(5), 2042–2051.

648 Havens, K., Kramer, A. T., & Guerrant Jr, E. O. (2014). Getting plant conservation right (or not):
649 The case of the United States. *International Journal of Plant Sciences*, *175*(1), 3–10.

650 Hjort, J. (1914). *Fluctuations in the great fisheries of northern Europe viewed in the light of*
651 *biological research*.

652 Holmes, E. E., Sabo, J. L., Viscido, S. V., & Fagan, W. F. (2007). A statistical approach to
653 quasi-extinction forecasting. *Ecology Letters*, *10*(12), 1182–1198.

654 Holmes, E. E., Ward, E. J., & Scheuerell, M. D. (2014). Analysis of multivariate time-series
655 using the MARSS package. *NOAA Fisheries, Northwest Fisheries Science Center*, *2725*,
656 98112.

657 Holmes, E., & Semmens, B. (2004). Viability analysis for endangered metapopulations: A
658 diffusion approximation approach. In *Ecology, genetics and evolution of metapopulations*
659 (pp. 565–597). Elsevier.

660 Hovel, R. A., Carlson, S. M., & Quinn, T. P. (2017). Climate change alters the reproductive
661 phenology and investment of a lacustrine fish, the three-spine stickleback. *Global*
662 *Change Biology*, *23*(6), 2308–2320.

663 Hyndman, R. J., Athanasopoulos, G., Bergmeir, C., Caceres, G., Chhay, L., O'Hara-Wild, M.,
664 Petropoulos, F., Razbash, S., & Wang, E. (2020). Package 'forecast.' *Online]*
665 *Https://Cran. r-Project. Org/Web/Packages/Forecast/Forecast. Pdf*.

666 IPBES, W. (2019). Intergovernmental science-policy platform on biodiversity and ecosystem
667 services. *Summary for Policy Makers of the Global Assessment Report on Biodiversity*
668 *and Ecosystem Services of the Intergovernmental Science-Policy Platform on*
669 *Biodiversity and Ecosystem Services. IPBES Secretariat, Bonn, Germany*.

670 Jachowski, D. S., Butler, A., Eng, R. Y., Gigliotti, L., Harris, S., & Williams, A. (2020). Identifying
671 mesopredator release in multi-predator systems: A review of evidence from North
672 America. *Mammal Review*, *50*(4), 367–381.

673 Jenkins, G. P., Coleman, R. A., Barrow, J. S., & Morrongiello, J. R. (2022). Environmental
674 drivers of fish population dynamics in an estuarine ecosystem of south-eastern Australia.
675 *Fisheries Management and Ecology*, *29*(5), 693–707.

676 Jha, B., Nath, D., Srivastava, N., & Satpathy, B. (2008). Estuarine fisheries management
677 options and strategies. *CIFRI Policy Papers*, *3*, 1–23.

678 Kimmerer, W. J., Gartside, E., & Orsi, J. J. (1994). Predation by an introduced clam as the likely
679 cause of substantial declines in zooplankton of San Francisco Bay. *Marine Ecology*
680 *Progress Series*, 81–93.

681 Knape, J., & de Valpine, P. (2011). Effects of weather and climate on the dynamics of animal
682 population time series. *Proceedings of the Royal Society B: Biological Sciences*,
683 *278*(1708), 985–992.

684 Koeller, P., Fuentes-Yaco, C., Platt, T., Sathyendranath, S., Richards, A., Ouellet, P., & Aschan,
685 M. (2009). Basin-scale coherence in phenology of shrimps and phytoplankton in the
686 North Atlantic Ocean. *Science*, *324*(5928), 791–793.

687 Komoroske, L., Connon, R., Lindberg, J., Cheng, B., Castillo, G., Hasenbein, M., & Fangue, N.
688 (2014). Ontogeny influences sensitivity to climate change stressors in an endangered
689 fish. *Conservation Physiology*, *2*(1), cou008.

690 Lane, P. A. (1975). The dynamics of aquatic systems: A comparative study of the structure of
691 four zooplankton communities. *Ecological Monographs*, *45*(4), 307–336.

692 Langan, J. A., Puggioni, G., Oviatt, C. A., Henderson, M. E., & Collie, J. S. (2021). *Climate*
693 *alters the migration phenology of coastal marine species* (Marine Ecology Progress
694 Series, Vol. 660, pp. 1–18).

695 Lauchlan, S. S., & Nagelkerken, I. (2020). Species range shifts along multistressor mosaics in
696 estuarine environments under future climate. *Fish and Fisheries*, *21*(1), 32–46.

697 Lawrence, R. K., Mattson, W. J., & Haack, R. A. (1997). White spruce and the spruce budworm:
698 Defining the phenological window of susceptibility. *The Canadian Entomologist*, *129*(2),
699 291–318.

700 Mac Nally, R., Thomson, J. R., Kimmerer, W. J., Feyrer, F., Newman, K. B., Sih, A., Bennett, W.
701 A., Brown, L., Fleishman, E., & Culberson, S. D. (2010). Analysis of pelagic species
702 decline in the upper San Francisco Estuary using multivariate autoregressive modeling
703 (MAR). *Ecological Applications*, *20*(5), 1417–1430.

704 Marques, S. C., Azeiteiro, U. M., Marques, J. C., Neto, J. M., & Pardal, M. Â. (2006).
705 Zooplankton and ichthyoplankton communities in a temperate estuary: Spatial and
706 temporal patterns. *Journal of Plankton Research*, *28*(3), 297–312.

707 Mawdsley, J. R., O'MALLEY, R., & Ojima, D. S. (2009). A review of climate-change adaptation
708 strategies for wildlife management and biodiversity conservation. *Conservation Biology*,
709 *23*(5), 1080–1089.

710 Morrongiello, J. R., Walsh, C. T., Gray, C. A., Stocks, J. R., & Crook, D. A. (2014).
711 Environmental change drives long-term recruitment and growth variation in an estuarine
712 fish. *Global Change Biology*, *20*(6), 1844–1860.

713 Nobriga, M. L., & Feyrer, F. (2008). Diet composition in San Francisco Estuary striped bass:
714 Does trophic adaptability have its limits? *Environmental Biology of Fishes*, *83*, 495–503.

O'Gorman, E. J., & Emmerson, M. C. (2009). Perturbations to trophic interactions and the stability of complex food webs. *Proceedings of the National Academy of Sciences*, *106*(32), 13393–13398.

Otero, J., L'Abée-Lund, J. H., Castro-Santos, T., Leonardsson, K., Storvik, G. O., Jonsson, B., & Vøllestad, L. A. (2014). Basin-scale phenology and effects of climate variability on global timing of initial seaward migration of Atlantic salmon (Salmo salar. *Global Change Biology*, *20*(1), 61–75.

Ovaskainen, O., Skorokhodova, S., Yakovleva, M., Sukhov, A., Kutenkov, A., Kutenkova, N., & Delgado, M. D. M. (2013). Community-level phenological response to climate change. *Proceedings of the National Academy of Sciences*, *110*(33), 13434–13439.

Pak, N., Colombano, D. D., Greiner, T., Hobbs, J. A., Carlson, S. M., & Ruhi, A. (2023). Disentangling abiotic and biotic controls of age-0 Pacific herring population stability across the San Francisco Estuary. *Ecosphere*, *14*(5), e4440.

Peterson, C. D., Parsons, K. T., Bethea, D. M., Driggers III, W. B., & Latour, R. J. (2017). Community interactions and density dependence in the southeast United States coastal shark complex. *Marine Ecology Progress Series*, *579*, 81–96.

Potts, W., Bealey, R., & Childs, A. (2016). Assessing trophic adaptability is critical for understanding the response of predatory fishes to climate change: A case study of Pomatomus saltatrix in a global hotspot. *African Journal of Marine Science*, *38*(4), 539–547.

Qasim, S. Z., Bhattathiri, P. M. A., & Devassy, V. P. (1972). The influence of salinity on the rate of photosynthesis and abundance of some tropical phytoplankton. *Marine Biology*, *12*, 200–206.

Quiñones, R. M., & Moyle, P. B. (2014). Climate change vulnerability of freshwater fishes of the San Francisco Bay area. *San Francisco Estuary and Watershed Science*, *12*(3).

Reis, G. J., Howard, J. K., & Rosenfield, J. A. (2019). Clarifying effects of environmental protections on freshwater flows to—And water exports from—The San Francisco Bay estuary. *San Francisco Estuary and Watershed Science*, *17*(1).

743 Robins, P. E., Skov, M. W., Lewis, M. J., Giménez, L., Davies, A. G., Malham, S. K., Neill, S. P.,
744 McDonald, J. E., Whitton, T. A., & Jackson, S. E. (2016). Impact of climate change on
745 UK estuaries: A review of past trends and potential projections. *Estuarine, Coastal and*
746 *Shelf Science*, *169*, 119–135.

747 Rose, K. A., Kimmerer, W. J., Edwards, K. P., & Bennett, W. A. (2013). Individual-based
748 modeling of Delta Smelt population dynamics in the upper San Francisco Estuary: I.
749 Model description and baseline results. *Transactions of the American Fisheries Society*,
750 *142*(5), 1238–1259.

751 Rosenfield, J. A., & Baxter, R. D. (2007). Population dynamics and distribution patterns of
752 longfin smelt in the San Francisco Estuary. *Transactions of the American Fisheries*
753 *Society*, *136*(6), 1577–1592.

754 Ruhi, A., Dong, X., McDaniel, C. H., Batzer, D. P., & Sabo, J. L. (2018). Detrimental effects of a
755 novel flow regime on the functional trajectory of an aquatic invertebrate metacommunity.
756 *Global Change Biology*, *24*(8), 3749–3765.

757 Ruhí, A., Olden, J. D., & Sabo, J. L. (2016). Declining streamflow induces collapse and
758 replacement of native fish in the American Southwest. *Frontiers in Ecology and the*
759 *Environment*, *14*(9), 465–472.

760 Sabo, J. L. (2008). Population viability and species interactions: Life outside the single-species
761 vacuum. *Biological Conservation*, *141*(1), 276–286.

762 Sanford, E., Sones, J. L., García-Reyes, M., Goddard, J. H., & Largier, J. L. (2019). Widespread
763 shifts in the coastal biota of northern California during the 2014–2016 marine heatwaves.
764 *Scientific Reports*, *9*(1), 4216.

765 Sarremejane, R., Stubbington, R., England, J., Sefton, C. E., Eastman, M., Parry, S., & Ruhi, A.
766 (2021). Drought effects on invertebrate metapopulation dynamics and quasi-extinction
767 risk in an intermittent river network. *Global Change Biology*, *27*(17), 4024–4039.

768 Scanes, E., Scanes, P. R., & Ross, P. M. (2020). Climate change rapidly warms and acidifies
769 Australian estuaries. *Nature Communications*, *11*(1), 1803.

See, K. E., & Holmes, E. E. (2015). Reducing bias and improving precision in species extinction forecasts. *Ecological Applications*, *25*(4), 1157–1165.

Seifert, L. I., Weithoff, G., Gaedke, U., & Vos, M. (2015). Warming-induced changes in predation, extinction and invasion in an ectotherm food web. *Oecologia*, *178*, 485–496.

Simenstad, C. A., Fresh, K. L., & Salo, E. O. (1982). The role of Puget Sound and Washington coastal estuaries in the life history of Pacific salmon: An unappreciated function. In *Estuarine comparisons* (pp. 343–364). Academic Press.

Smith, R. L. (1974). Life history of Abedus herberti in central Arizona (Hemiptera: Belostomatidae. *Psyche: A Journal of Entomology*, *81*, 272–283.

Sommer, T., Armor, C., Baxter, R., Breuer, R., Brown, L., Chotkowski, M., Culberson, S., Feyrer, F., Gingras, M., & Herbold, B. (2007). The collapse of pelagic fishes in the upper San Francisco Estuary: El colapso de los peces pelagicos en la cabecera del Estuario San Francisco. *Fisheries*, *32*(6), 270–277.

Stenseth, N. C., & Mysterud, A. (2002). Climate, changing phenology, and other life history traits: Nonlinearity and match–mismatch to the environment. *Proceedings of the National Academy of Sciences*, *99*(21), 13379–13381.

Swaisgood, R. R. (2007). Current status and future directions of applied behavioral research for animal welfare and conservation. *Applied Animal Behaviour Science*, *102*(3–4), 139–162.

Tempel, T. L., Malinich, T. D., Burns, J., Barros, A., Burdi, C. E., & Hobbs, J. A. (2021). The value of long-term monitoring of the San Francisco Estuary for delta smelt and longfin smelt. *Calif Fish Game*, *107*, 148–171.

Thakur, M. P. (2020). Climate warming and trophic mismatches in terrestrial ecosystems: The green–brown imbalance hypothesis. *Biology Letters*, *16*(2), 20190770.

USFWS (2024). Docket No. FWS–R8–ES–2022–0082.

Varpe, Ø., & Fiksen, Ø. (2010). Seasonal plankton–fish interactions: Light regime, prey phenology, and herring foraging. *Ecology*, *91*(2), 311–318.

Vasseur, D. A., & Fox, J. W. (2009). Phase-locking and environmental fluctuations generate synchrony in a predator–prey community. *Nature*, *460*(7258), 1007–1010.

Visser, M. (2022). Phenology: Climate change is shifting the rhythm of nature. In *Frontiers 2022: Noise, Blazes and Mismatches: Emerging Issues of Environmental Concern* (pp. 41–58). United Nations Environment Programme (UNEP).

Ward, E. J., Chirakkal, H., González-Suárez, M., Aurioles-Gamboa, D., Holmes, E. E., & Gerber, L. (2010). Inferring spatial structure from time-series data: Using multivariate state-space models to detect metapopulation structure of California sea lions in the Gulf of California, Mexico. *Journal of Applied Ecology*, *47*(1), 47–56.

Werner, E. E., & Gilliam, J. F. (1984). The ontogenetic niche and species interactions in size-structured populations. *Annual Review of Ecology and Systematics*, *15*, 393–425.

Winemiller, K. O., & Rose, K. A. (1992). Patterns of life-history diversification in North American fishes: Implications for population regulation. *Canadian Journal of Fisheries and Aquatic Sciences*, *49*(10), 2196–2218.

Winemiller, K. O., & Rose, K. A. (1993). Why do most fish produce so many tiny offspring? *The American Naturalist*, *142*(4), 585–603.

Young, M. J., Feyrer, F., Smith, C. D., & Valentine, D. A. (2022). Habitat-specific foraging by striped bass (Morone saxatilis) in the San Francisco Estuary, California: Implications for tidal restoration. *San Francisco Estuary and Watershed Science*, *20*(3).

Zhemchuzhnikov, M. K., Versluijs, T. S., Lameris, T. K., Reneerkens, J., Both, C., & van Gils, J. A. (2021). Exploring the drivers of variation in trophic mismatches: A systematic review of long-term avian studies. *Ecology and Evolution*, *11*(9), 3710–3725.

Figures

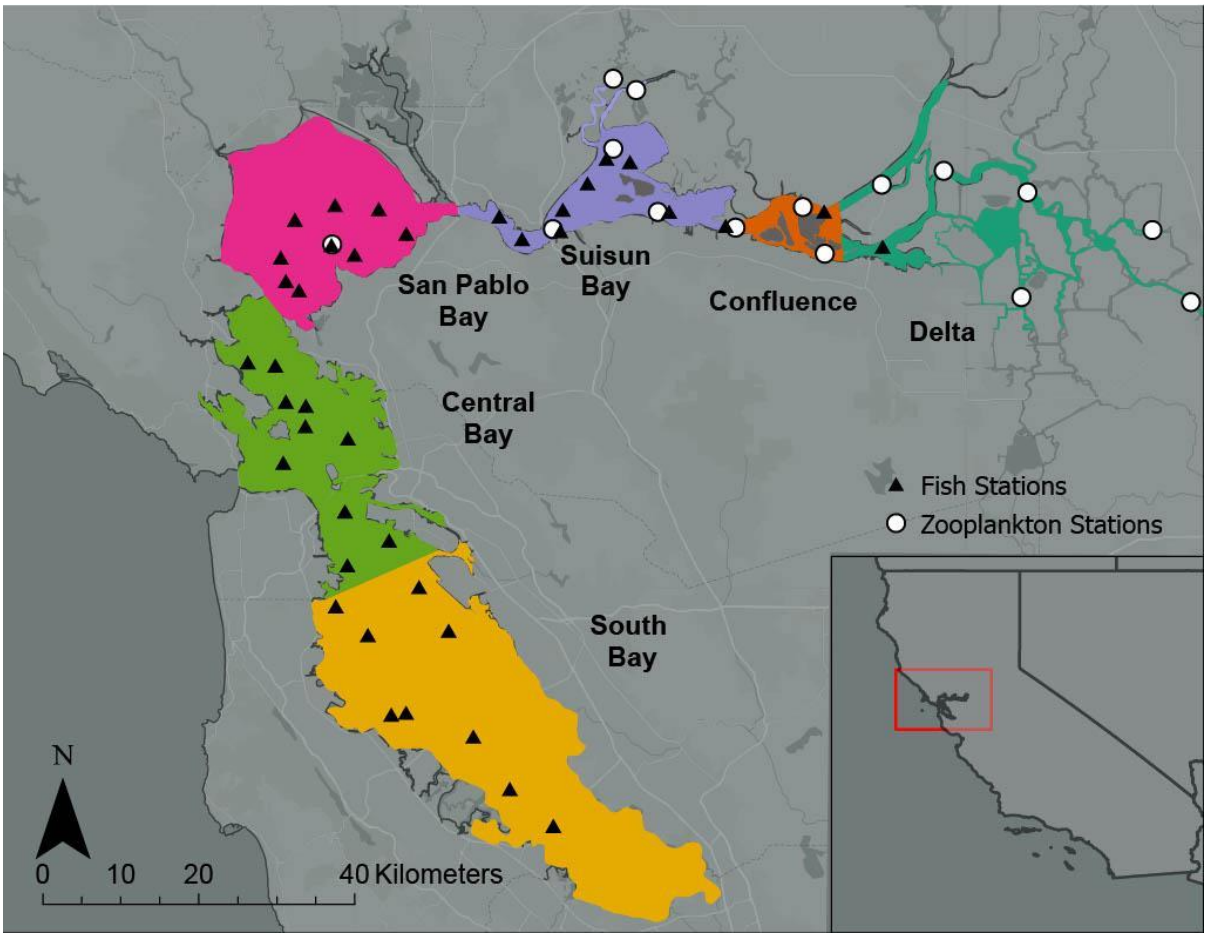

Figure 1: Map of the San Francisco Estuary, California, USA. Regions are shown as color-coded polygons, with core fish and zooplankton sampling stations shown as black triangles and white circles, respectively. Along the longitudinal axis of the estuarine gradient, and depending on hydroclimatic conditions, salinity can range from polyhaline (18-30 PSU in the Central Bay, which is connected to the Pacific Ocean) to brackish and fresh (0-5 PSU in the Delta).

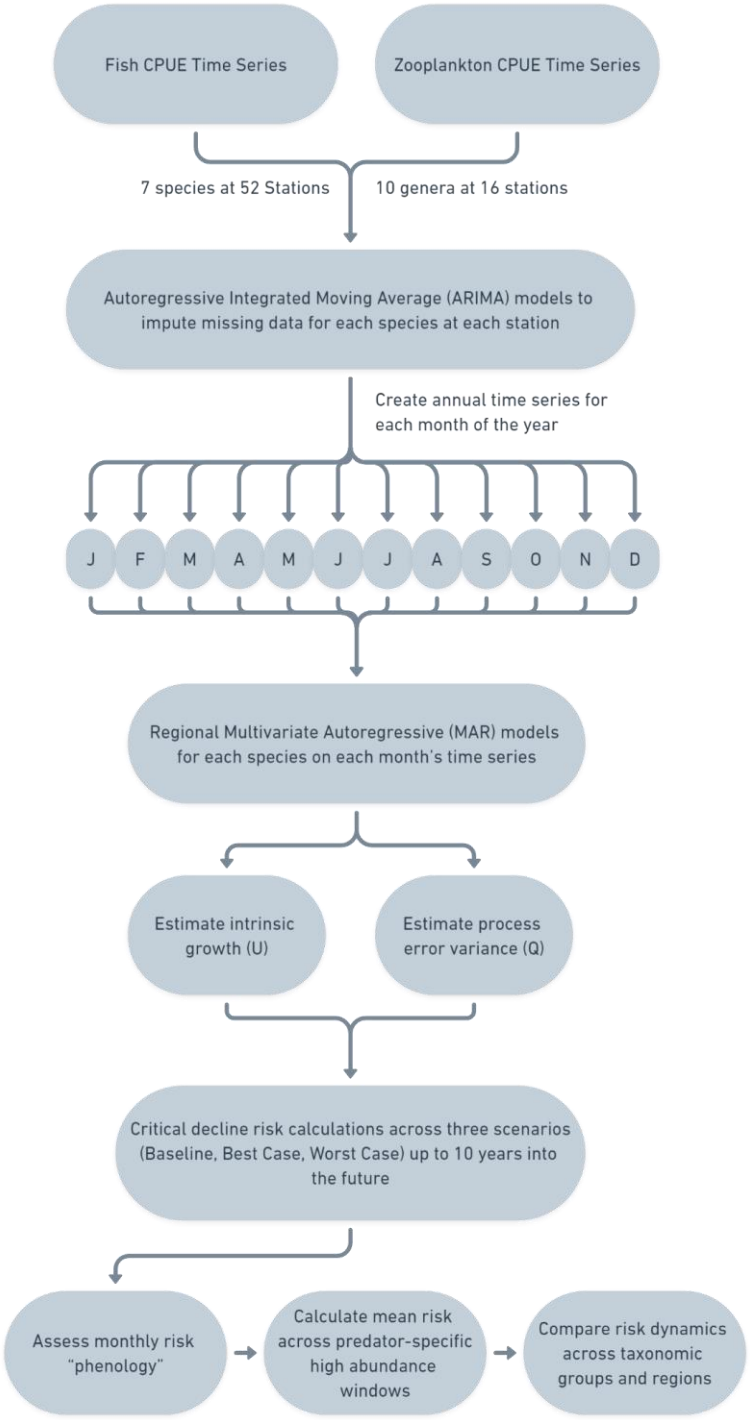

Figure 2: Flow chart of analyses. We illustrate the data inputs, series modeling steps, and critical decline risk outputs.

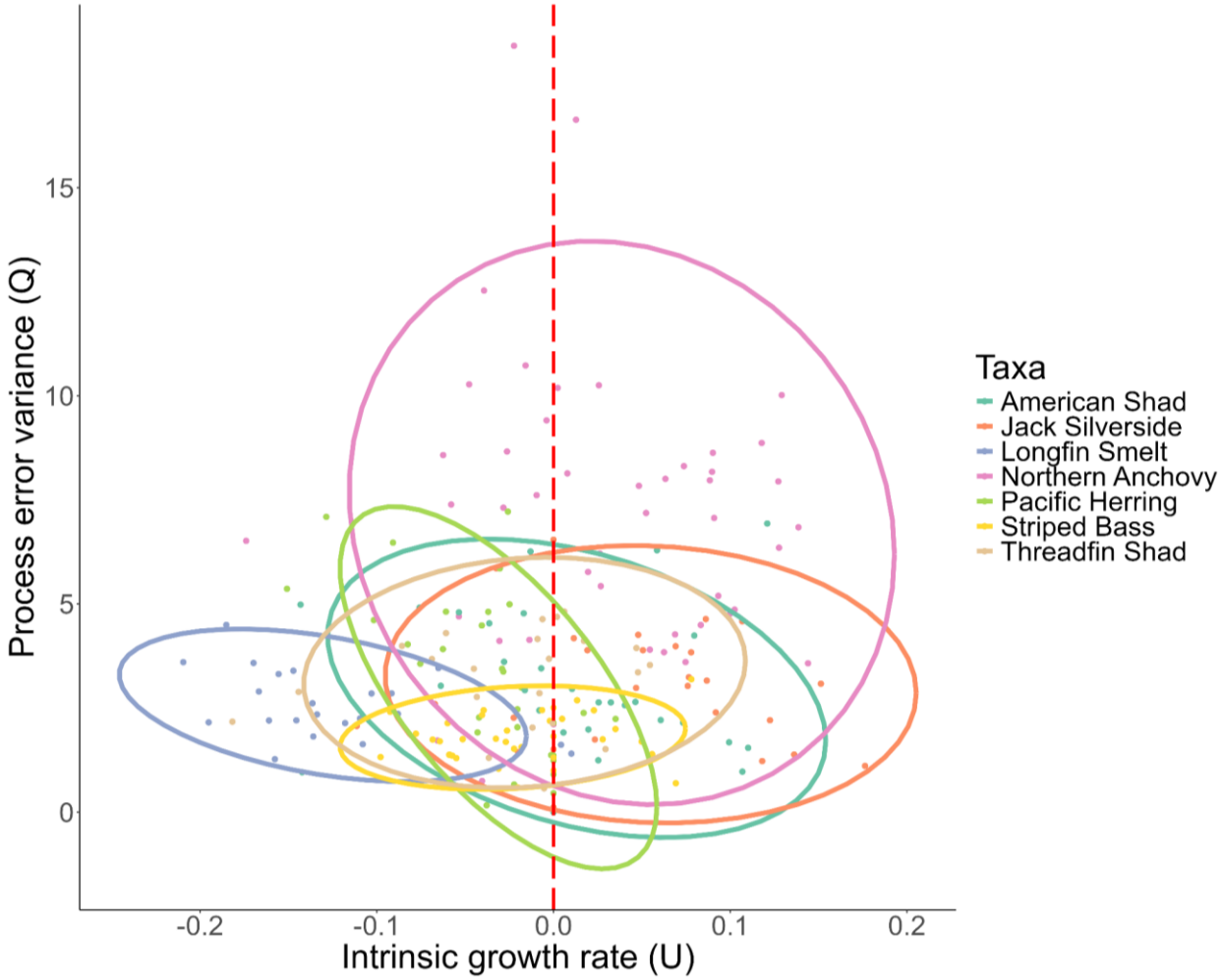

Figure 3: Diversity of population trajectories within and across species. The biplot represents Intrinsic growth rates (*U*), versus estimated process error variance (*Q*) estimated by the Multivariate Autoregressive (MAR) models. For growth rates, values below zero indicate year-to-year declines in population estimates for that month and region, while values above zero indicate positive trends. For process error variance, higher values indicate stronger year-to-year fluctuations in population estimates for that month and region. Each point represents a species in a given region for each month of the year. We fitted standard ellipses to each species to display the diversity of species-level trajectories. See Figure S2 in the supplementary for additional visualizations of these data.

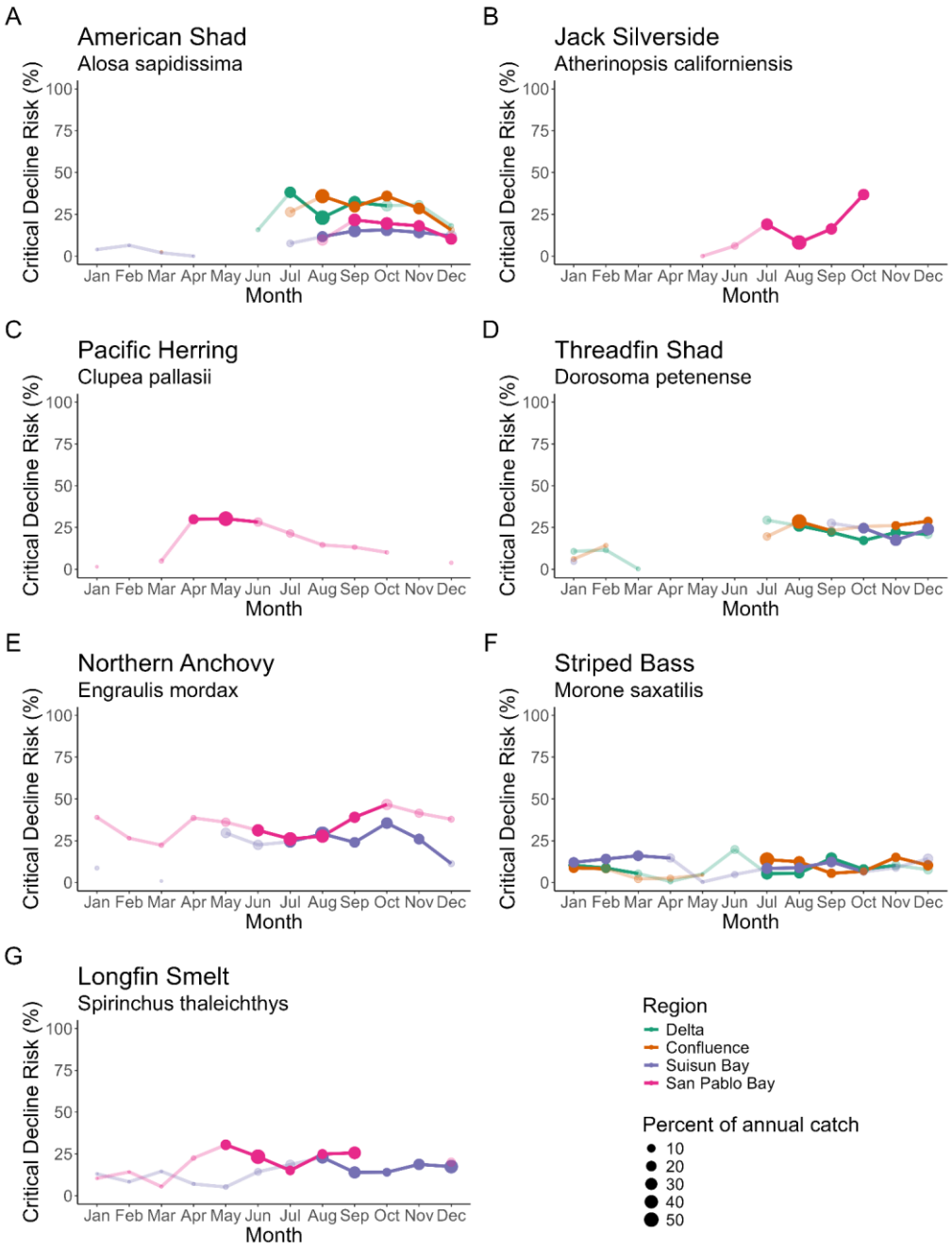

Figure 4: Phenology of risk. Monthly risk that an age-0 fish species would experience a 90% population decline for that month in each region. Points are scaled by percentage of mean annual catch. High abundance windows–i.e., months that contain 80% of the mean annual catch–are in saturated tones while off-window months are desaturated. Gaps indicate that a species often had zero abundance for that month and region and were thus not modeled.

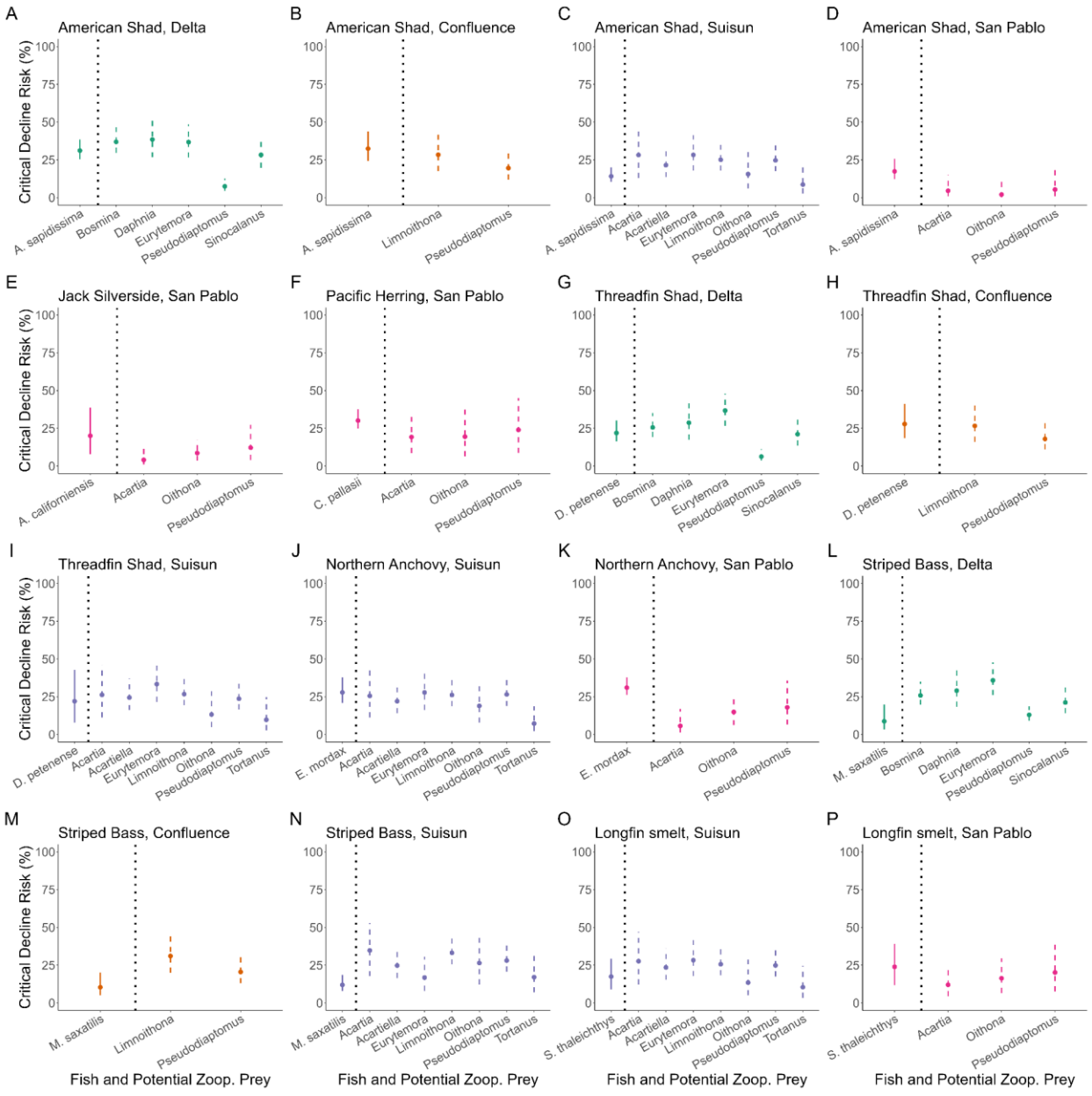

Figure 5: Mean critical decline risk of fish during their high-abundance windows paired with the potential suite of zooplankton prey within that same window. Points represent probabilities calculated from maximum likelihood parameter estimates. Lower bound represents "best case scenario" wherein decline risks are calculated with the most positive population trend and lowest amount of process error variance. Upper bound represents "worst case scenario" calculated with the most negative population trend and highest amount of process error variance.

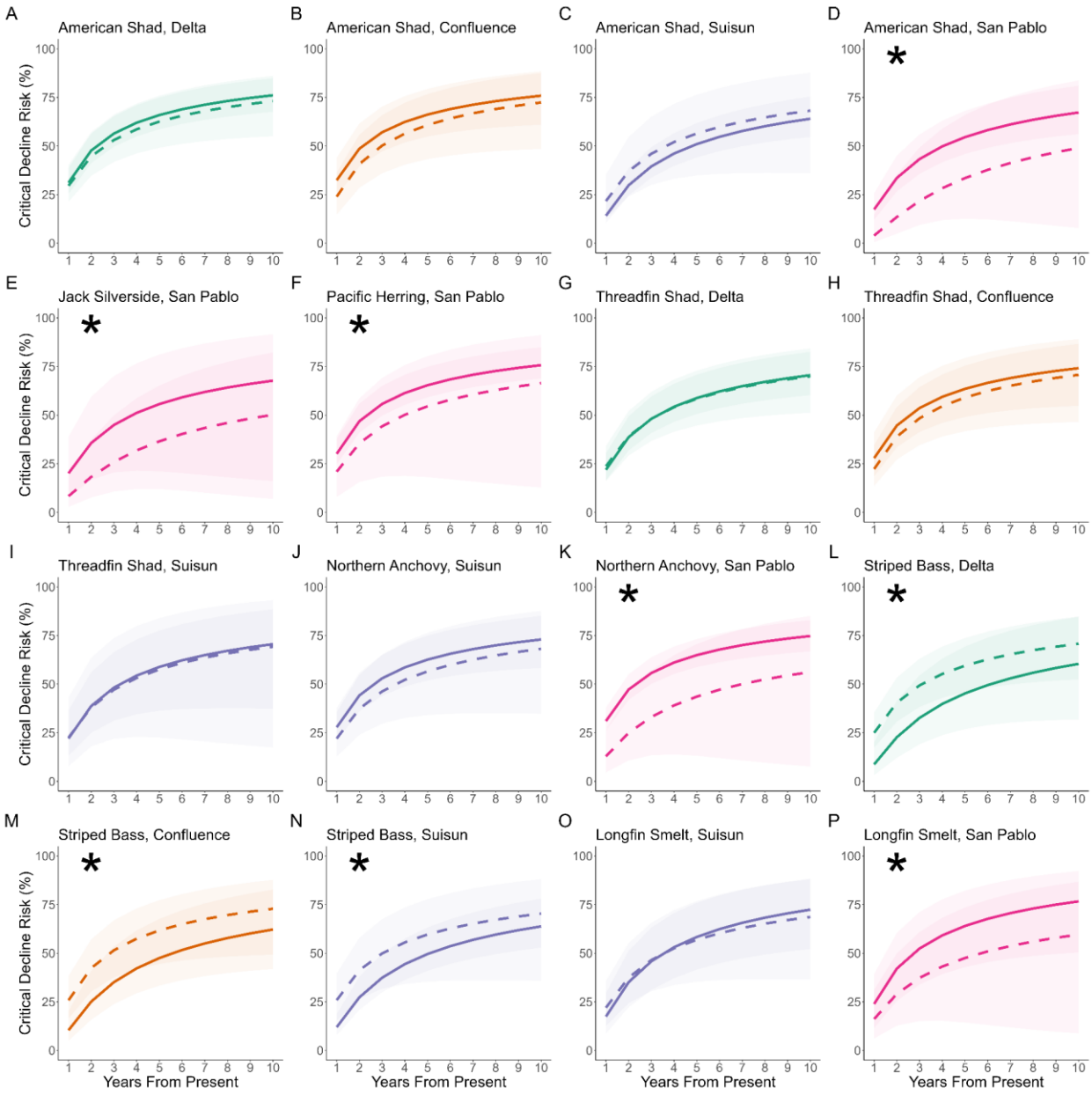

Figure 6: Projection of critical decline risk 10 years into the future. We projected out 10 years from present for fish predators (solid line) in their high population window and the mean risk of their zooplankton prey assemblage (dashed line) during that same window. Bands represent the range between best case and worst case scenarios. Asterisks represent significant differences between fishes and zooplankton (American Shad, $F_{1,5.891}$, p=0.0161; Threadfin Shad, $F_{1,0.145}$, p=0.710, Jack Silverside, $F_{1,16.245}$, p<0.001; Pacific Herring, $F_{1,8.435}$, p=0.0062; Northern Anchovy, $F_{1,12.214}$, p<0.001; Striped Bass, $F_{1,40.244}$, p<0.001; Longfin Smelt, $F_{1,4.173}$, p=0.043).

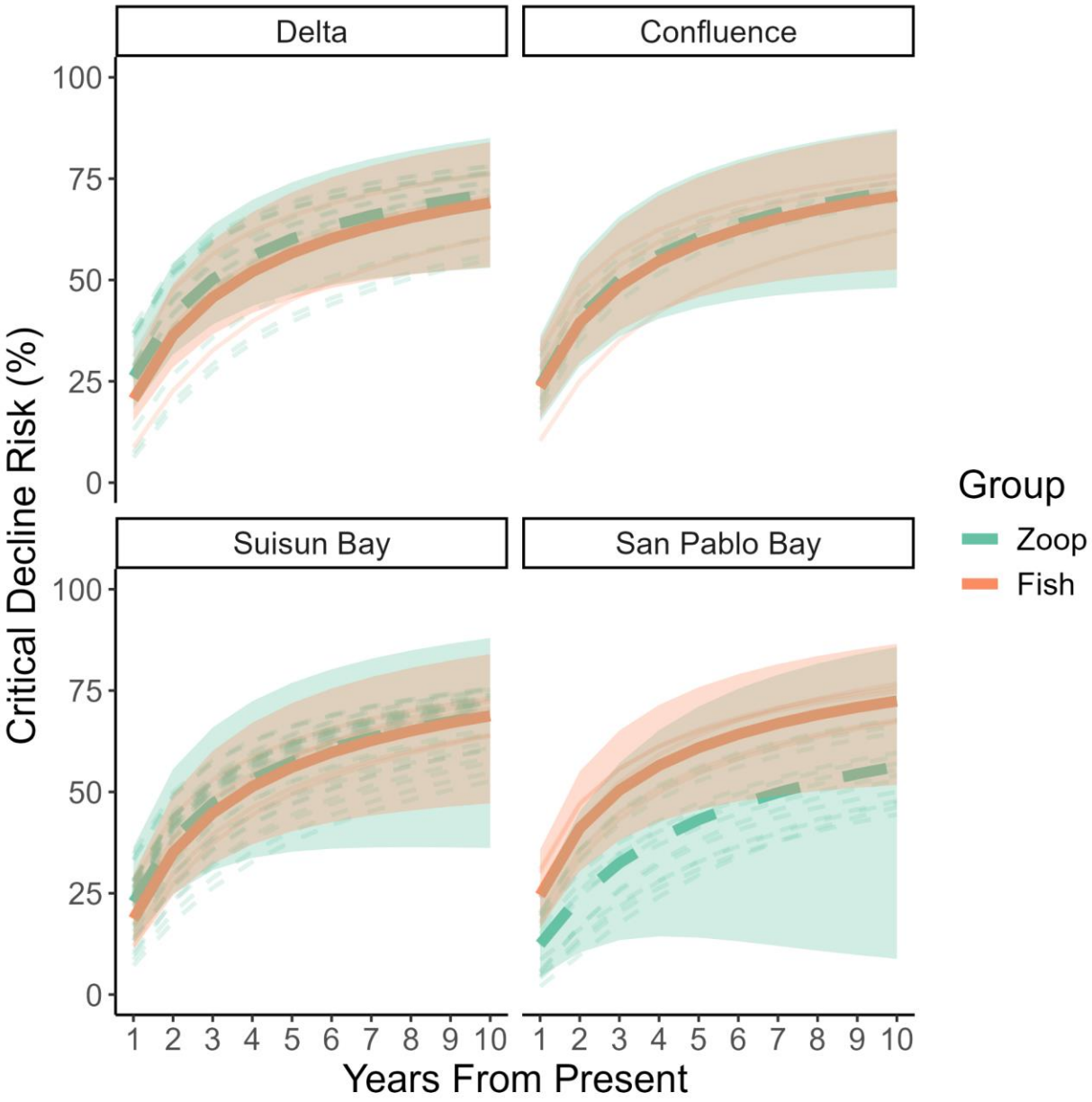

Figure 7: Accumulation of community-wide risk across regions of the estuary. We display mean decline risk for all predators (orange, solid line) and their paired prey assemblages (green, dashed line) in each region during high abundance windows projected out for 10 years. Individual taxa are represented by desaturated lines. Bands represent the mean range between best case and worst case scenarios (see methods for details).